Fully 3D multiple beam dynamics processes simulation for the Fermilab Tevatron

E Stern, J Amundson, P Spentzouris and A Valishev
Fermi National Accelerator Laboratory, P.O. Box 500, Batavia, IL, USA
E-mail: egstern@fnal.gov

Abstract. The Fermilab Tevatron has been, until 2010, the premier high-energy physics collider in the world. The data collected over the last decade by high-energy physics experiments running at the Tevatron have been analyzed to make important measurements in fundamental areas such as B meson masses and flavor oscillation, searches for the Higgs boson, and supersymmetry. Collecting these data at the limits of detectability has required the Tevatron to operate reliably at high beam intensities to maximize the number of collisions to analyze. This impressive achievement has been assisted by the use of HPC resources and software provided through the SciDAC program. This paper describes the enhancements to the `BeamBeam3d` code to realistically simulate the Tevatron, the validation of these simulations, and the improvement in equipment reliability and personal safety achieved with the aid of simulations.

1. Introduction

The task of asking and answering the most basic fundamental questions about the nature of time, space, matter and energy falls to the sciences of particle physics and astrophysics. The particle accelerator[1] is the main tool used by experimental particle physicists to create new forms of matter which are studied to understand their interactions and relationship with other well-understood matter. In pursuing new realms of interactions and new forms of matter, physicists use accelerators running at the highest possible energies. Running the accelerator at larger energies allows the exploration of previously unknown regimes through the production of more massive particles. Since the occurrence of new physics processes is likely to be rare, the accelerator has to generate interactions at a high rate so that sufficient numbers of new particles may be produced and identified. In accelerator physics, this is referred to as running with high luminosity.

For the last decade until 2010, the Tevatron operating at the Fermi National Accelerator Laboratory has been the highest energy accelerator in the world. The Fermilab Tevatron [2] is a collider accelerator in which beams of protons and antiprotons circulate in opposite directions and collide at a center-of-mass energy of 1.96 TeV.

Accelerators are large complicated devices. Throughout physical length of the Tevatron, (see Fig. 1) which exceeds six kilometers, thousands of magnets for steering and focusing charged particles, radio-frequency cavities for acceleration and bunch shaping, along with the ancillary support equipment including vacuum, cryogenic, power, cooling and diagnostic equipment are assembled and work together in the delicate task of capturing and accelerating beams made of 72 bunches of over 10^{13} mutually repelling charged particles, bringing them into collision while

Figure 1. View inside the Tevatron tunnel. Image courtesy of Fermilab Visual Media Services.

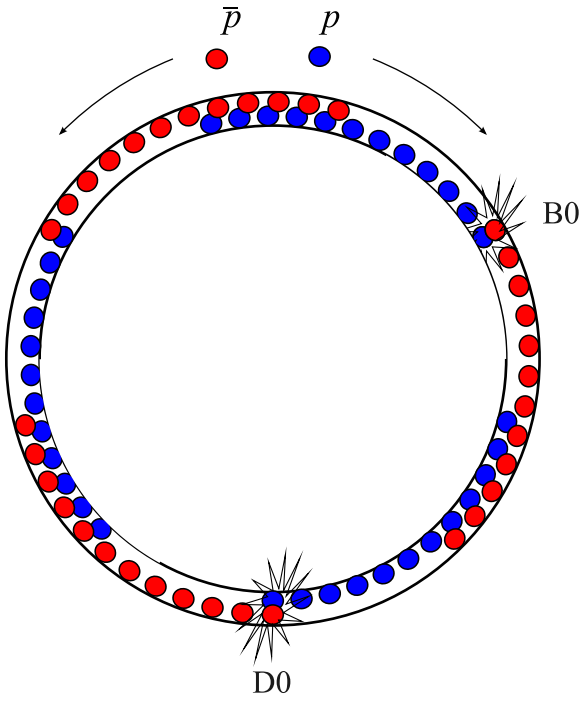

Figure 2. Schematic of the position of proton and antiproton bunches in the Tevatron with 36 proton and 36 antiproton bunches. The diagram shows the positions at a time when the lead bunch of the trains are at the head-on collision location. Head-on collisions occur at location B0 and D0.

maintaining the beams with minimal particle losses for hours at a time. Beams in accelerators are subject to dynamic physical processes which disrupt normal operations by causing instability and beam loss. The strength of these disruptive effects increases with increasing beam intensity, which interferes with the goal of running high luminosity beams for physics.

Each colliding beam consists of 36 bunches of particles shown schematically in Fig. 2. The proton and antiproton beams circulate in opposite directions around the ring moving in a common vacuum pipe. For high-energy physics operations, the beams collide head-on at the B0 and D0 interaction points (IPs) which are surrounded by particle detectors. In the intervening arcs the beams are separated by means of electrostatic separators; long-range (also referred to as parasitic) collisions occur at 136 other locations. Head-on and long-range interactions couple

all of the bunches to each other, allowing the possibility of the development of coherent modes of oscillation. The magnetic optics of the horizontal and vertical planes of the Tevatron are strongly coupled, so perturbations in one plane will appear in the other plane. The charged beams also interact electromagnetically with the conducting walls of the vacuum chamber, introducing an impedance effect which distorts and perturbs the bunches. The focusing strength of the magnetic elements in the beamline varies with particle momentum, an effect called chromaticity, which can contribute to, or dampen, the development of impedance driven instabilities[9]. The combination of impedance and beam-beam interactions could also lead to the development of dipole or quadrupole mode instabilities[5].

The combination of all these effects imposes serious limitations on machine operations, hence constant efforts are being exerted to better understand the beam dynamics. Due to the extreme complexity of the problem, a numerical simulation appears to be one of the most reliable ways to study performance of the system. A simulation that takes into account the number of bunches (72), the number of macroparticles needed for a faithful rendering of bunch characteristics (> 500000), and the number of interaction regions (~ 100) can only be performed with high performance computing using optimized algorithms for calculating collective electromagnetic effects amongst many charged particles.

This paper presents a macroparticle simulation that includes the main features essential for studying the coherent motion of bunches in a collider: a self-consistent 3D Poisson solver for beam-beam force computation, multiple bunch tracking with the complete account of sequence and location of long-range and head-on collision points, and a machine model including our measurement based understanding of the coupled linear optics, chromaticity, and resistive wall impedance.

We validate individual physical processes against measured data where possible, and analytic calculations elsewhere. Finally, we present simulations of the effects of increasing beam intensity with single and multiple bunches, and study the combined effect of long-range beam-beam interactions and transverse impedance. The results of the simulations were successfully used in Tevatron operations to support a change of chromaticity during the transition to collider mode optics leading to a factor of two decrease in proton losses. This allowed the Tevatron to run with with higher intensity while remaining within radiation safety margins, improving reliability of collider operations and the physics discovery potential of the machine.

2. BeamBeam3d code

The Poisson solver in the `BeamBeam3d` code is described in Ref. [6]. Two beams are simulated with macroparticles generated with a random distribution in phase space. The accelerator ring is conceptually divided into arcs with potential interaction points at the ends of the arcs. The optics of each arc is modeled with a 6×6 linear map that transforms the phase space $\{x, x', y, y', z, \delta\}$ coordinates of each macroparticle from one end of the arc to the other. There is significant coupling between the horizontal and vertical transverse coordinates in the Tevatron. For our Tevatron simulations, the maps were calculated using coupled lattice functions [7] obtained by fitting a model [8] of beam element configuration to beam position measurements. The longitudinal portion of the map produces synchrotron motion among the longitudinal coordinates with the frequency of the synchrotron tune. Chromaticity results in an additional momentum-dependent phase advance $\delta\mu_{x(y)} = \mu_0 C_{x(y)} \Delta p/p$, where $C_{x(y)}$ is the normalized chromaticity for x (or y) and μ_0 is the design phase advance for the arc. This is a generalization of the definition of chromaticity to apply to an arc, and reduces to the normalized chromaticity $(\Delta\nu/\nu)/(\Delta p/p)$ when the arc encompasses the whole ring. The additional phase advance is applied to each particle in the decoupled coordinate basis so that symplecticity is preserved.

The Tevatron includes electrostatic separators to generate a helical trajectory for the oppositely charged beams. The mean beam offset at the IP is included in the Poisson field

solver calculation. Different particle bunches are individually tracked through the accelerator. They interact with each other in the pattern and locations that they would have in the actual collider.

The impedance model applies a momentum kick to the particles generated by the dipole component of resistive wall wakefields [9]. Each beam bunch is divided longitudinally into slices containing approximately equal numbers of particles. As each bunch is transported through an arc, particles in slice i receive a transverse kick from the resistive wall wake field induced by the dipole moment of the particles in forward slice j:

$$\frac{\Delta\vec{p}_\perp}{p} = \frac{2}{\pi b^3}\sqrt{\frac{4\pi\epsilon_0 c}{\sigma}}\ \frac{N_j r_0 <\vec{r}_j>}{\beta\gamma}\frac{L}{\sqrt{z_{ij}}} \tag{1}$$

The length of the arc is L, N_j is the number of particles in slice j, r_0 is the classical electromagnetic radius of the beam particle $e^2/4\pi\epsilon_0 m_0 c^2$, z_{ij} is the longitudinal distance between the particle in slice i that suffers the wakefield kick and slice j that induces the wake. $\vec{r}_j$ is the mean transverse position of particles in slice j, b is the pipe radius, c is the speed of light, σ is the conductivity of the beam pipe and $\beta\gamma$ are Lorentz factors of the beam. Quantities with units are specified in the MKSA system.

3. Synchrobetatron comparisons

We will assess the validity of the beam-beam calculation by comparing simulated synchrobetatron mode tunes with a measurement[10] performed at the VEPP-2M 500 MeV e^+e^- collider. These modes are an unambiguous marker of beam-beam interactions and provide a sensitive tool for evaluating calculational models. These modes arise in a colliding beam accelerator where the longitudinal bunch length and the transverse beta function are of comparable size. Particles at different z positions within a bunch are coupled through the electromagnetic interaction with the opposing beam leading to the development of coherent synchrobetatron modes. The tune shifts for different modes have a characteristic evolution with beam-beam parameter $\xi = Nr_0/4\pi\gamma\epsilon$, in which N is the number of particles, r_0 is the classical electromagnetic radius of the beam particle, and ϵ is the unnormalized one-sigma beam emittance.

There are two coherent transverse modes in the case of simple beam-beam collisions between equal intensity beams without synchrotron motion: the σ mode where the two beams oscillate with the same phase, and the π mode where the two beams oscillate with opposite phases [12]. Without synchrotron motion, the σ mode has the same tune as unperturbed betatron motion while the π mode frequency is offset by $K\xi$, where the parameter K is approximately equal to, but greater than 1 and depends on the transverse shape of the beams [11]. The presence of synchrotron motion introduces a more complicated spectrum of modes which are denoted by $n\sigma$ and $n\pi$ where n is the number of oscillation fixed-points along the bunch length induced by coupling.

We simulated the VEPP-2M collider using Courant-Snyder uncoupled maps. The horizontal emittance in the VEPP-2M beam is much larger than the vertical emittance. The bunch length (4 cm) is comparable to $\beta_y^* = 6$ cm so we expect to see synchrobetatron modes. In order to excite synchrobetatron modes, we set an initial y offset of one beam sigma approximately matching the experimental conditions.

Simulation runs with a range of beam intensities corresponding to beam-beam parameters of up to 0.015 were performed, in effect mimicking the experimental procedure described in Ref. [10]. For each simulation run, mode peaks were extracted from the Fourier transform of the mean bunch vertical position. The simulations were performed with 10^5 macroparticles per bunch. Doubling the number of macroparticles did not change the location or appearance of any

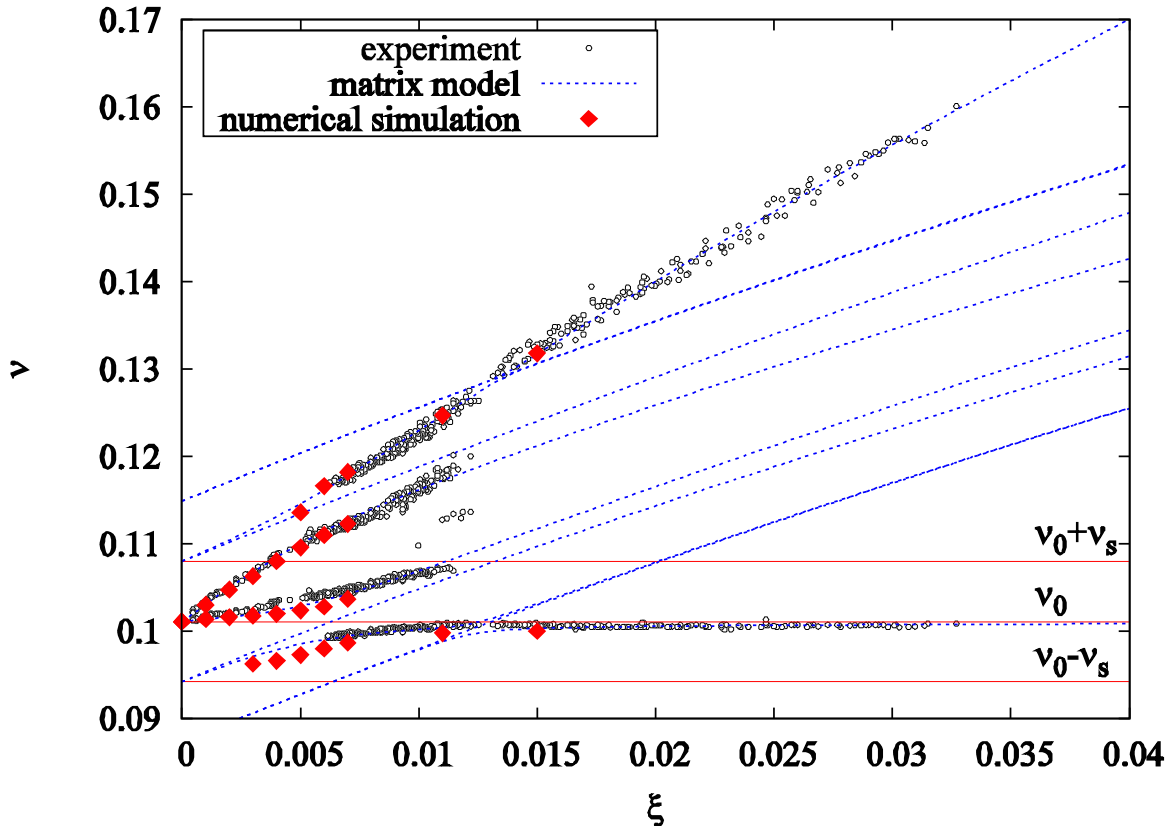

Figure 3. The points show the tunes of experimentally observed synchrobetatron modes at the VEPP-2M accelerator. The red diamonds show the tunes of simulated synchrobetatron modes as a function of beam-beam parameter ξ. The dashed lines show the evolution of mode frequencies predicted by the matrix model as described in the text.

mode peaks. In Fig. 3, we plot the mode peaks from the BeamBeam3d simulation as a function of ξ as red diamonds overlaid on experimental data from Ref. [10] and a phenomonelogical model using linearized coupled modes referred to as the matrix model described in Refs. [13, 14]. As can be seen, there is good agreement between the observation and simulation giving us confidence in the beam-beam calculation.

4. Impedance tests

Wakefields or, equivalently, impedance in an accelerator with a conducting vacuum pipe gives rise to well known instabilities. Our aim in this section is to demonstrate that the wakefield model in BeamBeam3d quantitatively reproduced these theoretically and experimentally well understood phenomena. Two instabilities considered are the strong and weak head-tail instability analyzed by Chao [15, 9]. These instabilities arise in extended length bunches in the presence of wakefields, synchrotron motion and betatron motion. The wakefield induced by the head of the bunch applies a driving force to the tail of the bunch that couples longitudinal motion to transverse motion. The coupling splits the beam oscillation frequency into upper and lower sidebands at frequencies $\nu_\beta + \nu_s$ and $\nu_\beta - \nu_s$. When he driving force is in-phase with the bunch's normal oscillation, the beam oscillations grow without damping.

The condition for the strong head-tail instability is that the strength of the in-phase driving

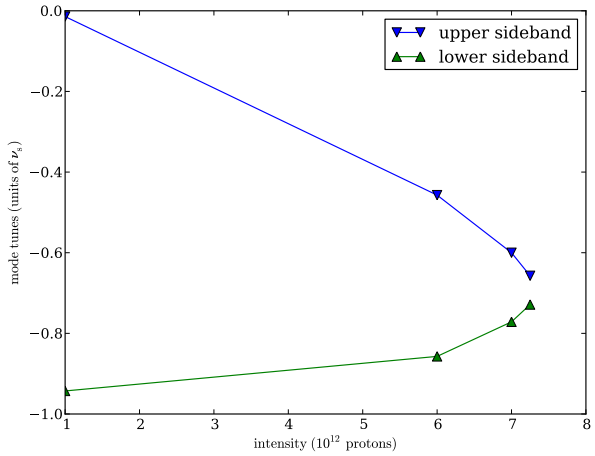

Figure 4. Evolution of the sideband mode frequencies as a function of beam intensity showing the two modes approaching a common frequency due to impedance. The y scale is in units of the synchrotron tune.

force (determined by beam intensity) overcomes the stabilizing effect of synchrotron motion. For any particular accelerator optical and geometric parameters, there is an intensity threshold above which the beam becomes unstable. As the beam intensity is increased, the two sidebands move closer to each other. At the point where they meet, the beam becomes unstable.

In Fig. 4, we show the evolution of the two modes as a function of beam intensity. With the tune and beam environment parameters of this simulation, Chao's two particle model predicts instability development at intensities of about 9×10^{12} particles, which is close to where the upper and lower modes meet. The model is derived assuming just a leading and trailing particle, while the simulation is done with the full particle distribution, altering the apparent strength of the wake function.

The interaction between impedance and chromaticity also causes a head-tail instability characterized by a parameter called the head-tail phase $\chi = 2\pi C\nu_\beta \hat{z}/c\eta$, where η is the slip factor of the machine and $\hat{z}$ is roughly the bunch length. The head-tail phase gives the size of betatron phase variation due to chromatic effects over the length of the bunch. Analysis by Chao[9] predicts a growth rate of

$$\tau^{-1} = \frac{Nr_0W_0}{2\pi\beta\gamma\nu_\beta}\chi \tag{2}$$

where N is the number of particles in the bunch, W_0 is the value of the wake function, β and γ are Lorentz factors and ν_β is the betatron tune and χ is the head-tail phase previously defined. Eqn. 2 predicts a growth rate that varies linearly with χ when the growth rate is normalized by the first factor, which includes all the beam intensity and geometric effects. The more detailed Vlasov analysis[16] also predicts a universal dependence of normalized growth rate versus head-tail phase that begins linearly with head-tail phase[16] and peaks around -1[1].

We simulated three different beam intensities with a range of chromaticites from $-.001$ to -0.5 to get head-tail phases in the 0 to -1 range. We extracted the growth rate from a logarithmic graph of the simulated beam size versus turn number and plot the normalized growth rate vs. head-tail phase in Fig. 5. The normalized curves are nearly identical and peak close to head-tail phase of unity. The deviation from a universal curve is again due to differences between the idealized model and detailed simulation.

We conclude that our simulation of resistive wall impedance is valid.

[1] The simulated machine is above transition (η is positive.) The head-tail instability develops when chromaticity is negative, thus the head-tail phase is negative.

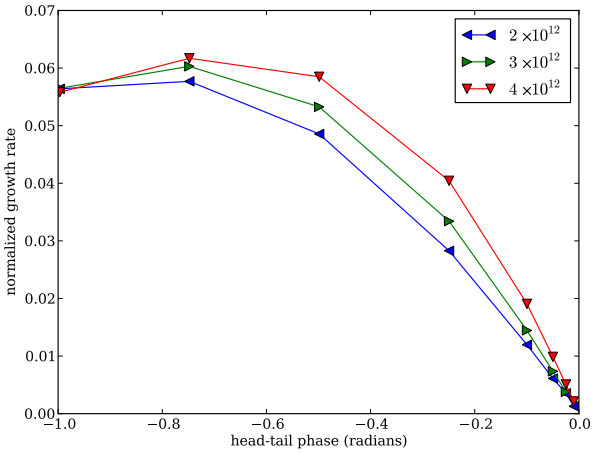

Figure 5. The normalized growth rate of dipole motion in the simulated accelerator with impedance and chromaticity as a function of head-tail phase χ at three beam intensities demonstrating their linear relationship close to 0 and the near-universal relationship for head-tail phase between -1 and 0.

5. Bunch-by-bunch emittance growth at the Tevatron

Referring back to Fig. 2, we see that there are three trains of twelve bunches for each species. A train occupies approximately 81.5° separated by a gap of about 38.5°. The bunch train and gap are replicated three times to fill the ring. Bunches collide head-on at the B0 and D0 interaction points but undergo long range (electromagnetic) beam-beam interactions at 136 other locations around the ring[2] although any particular bunch only has long range interactions at 70 of these locations.

Running the simulation with all 136 long-range IPs turns out to be very slow so we only calculated beam-beam forces at the two main IPs and the long-range IPs immediately upstream and downstream of them. The transverse beta functions at the long-range collision locations are much larger than the bunch length, so the beam-beam calculation at those locations can be performed using only the 2D solver.

One interesting consequence of the fill pattern and the helical trajectory is that any one of the 12 bunches in a train experiences collisions with the 36 bunches in the other beam at different locations around the ring, and in different transverse positions. This results in a different tune and emittance growth for each bunch of a train, but with the three-fold symmetry for the three trains. In the simulation, emittance growth arises from the effects of impedance acting on bunches that have been perturbed by beam-beam forces. The phenomenon of bunch dependent emittance growth is observed experimentally[17].

The beam-beam simulation with 36-on-36 bunches shows similar effects. We ran a simulation of 36 proton on 36 antiproton bunches for 50000 turns with the nominal helical orbit. The proton bunches had 8.8×10^{11} particles (roughly four times the usual number to enhance the effect) and the proton emittance was the typical 20π mm mrad. The antiproton bunch intensity and emittance were both half the corresponding proton bunch parameter. The initial emittance for each proton bunch was the same so changes during the simulation reflect the beam-beam effect.

Curve (a) in Figure 6 shows the emittance for each of the 36 proton bunches in a 36-on-36 simulation after 50000 turns of simulation. The three-fold symmetry is evident. The end bunches of the train (bunch 1, 13, 25) are clearly different from the interior bunches. For

[2] With three-fold symmetry of bunch trains, train-on-train collisions occur at six locations around the ring. The collision of two trains of 12 bunches each results in bunch-bunch collisions at 23 locations which, when multiplied by six, results in 138 collision points. It is a straightforward computer exercise to enumerate these locations. Two of these locations are distinguished as head-on while the remainder are parasitic.[17]

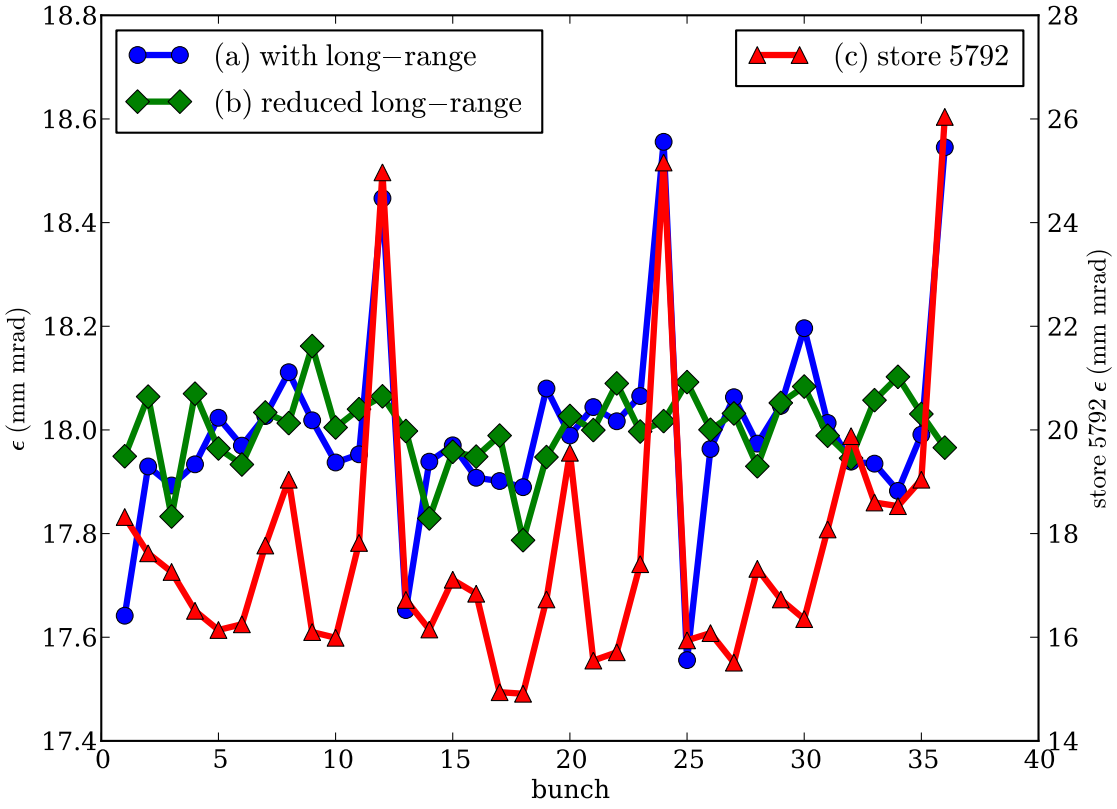

Figure 6. The simulated and measured emittance of each Tevatron proton bunch after running with 36 proton and 36 antiproton bunches. Curves (a) and (b) which show the emittance after 50000 simulated turns are read with the left vertical axis. Curve (a) results from a simulation with the nominal beam spacing at the long-range IPs. Curve (b) results from a simulation with the hypothetical condition where the beam separation at the long-range IPs is 100 times normal, suppressing the effect of those long-range IPs. Curve (c) is the measured emittance of bunches after 15 minutes of a particular store (#5792) of bunches in the Tevatron, and is read with the right vertical axis.

comparison, curve (c) shows the measured emittance taken during accelerator operations. The observed bunch emittance variation is similar to the simulation results. Another beam-beam simulation with the beam separation at the closest head-on IP expanded 100 times its nominal value resulted in curve (b) of Figure 6 showing a much reduced bunch-to-bunch variation. We conclude that the beam-beam effect at the long-range IPs is the origin of the bunch variation observed in the running machine and that our simulation of the beam helix is correct.

6. Lower chromaticity threshold

During the Tevatron operation in 2009 the limit for increasing the initial luminosity was determined by particle losses in the so-called squeeze phase [18]. At this stage the beams are separated in the main interaction points (not colliding head-on), and the machine optics is gradually changed to decrease the beta-function at these locations from 1.5 m to 0.28 m.

With proton bunch intensities currently approaching 3.2×10^{11} particles, the chromaticity of

the Tevatron has to be managed carefully to avoid the development of a head-tail instability. It was determined experimentally that after the head-on collisions are initiated, the Landau damping introduced by beam-beam interaction would be strong enough to maintain beam stability at chromaticity of +2 units (in Tevatron operations, chromaticity is $\Delta\nu/(\Delta p/p)$.) At the earlier stages of the collider cycle, when beam-beam effects are limited to long-range interactions the chromaticity was kept as high as 15 units since the concern was that the Landau damping is insufficient to suppress the instability. At the same time, high chromaticity causes particle losses which are often large enough to quench the superconducting magnets hence it is desireable to keep chromaticity at a reasonable minimum.

Table 1. Beam parameters for Tevatron simulation

Parameter	value
beam energy	980 GeV
p particles/bunch	3.0×10^{11}
$\bar{p}$ particles/bunch	0.9×10^{11}
p tune (ν_x, ν_y)	(20.585,20.587)
p (normalized) emittance	20π mm mrad
$\bar{p}$ tune (ν_x, ν_y)	(20.577,20.570)
$\bar{p}$ (normalized) emittance	6π mm mrad
synchrotron tune ν_s	0.0007
slip factor	0.002483
bunch length (rms)	43 cm
$\delta p/p$ momentum spread	1.2×10^{-4}
effective pipe radius	3 cm

Table 2. The azimuthal location (s), beam offset (D_x, D_y), and beta function (β_x, β_y) of the important long-range collision locations simulated in the study of chromaticity reduction in the Tevatron. During the setup for collisions, the beam separation is several bunch widths at the $B0$ and $D0$ locations (see Fig. 2) where head-on collisions would occur during collider operations.

s (m)		D_x (μm)	D_y (μm)	β_x (m)	β_y (m)
-59.28		258	-661	164.49	16.46
0.00	$B0$	-167	-16	0.33	0.37
59.28		642	292	19.74	155.64
2035.12		263	721	182.10	15.65
2094.40	$D0$	4	-171	0.29	0.35
2153.67		-639	222	19.32	147.45

Our multi-physics simulation was used to determine the safe lower limit for chromaticity. The simulations were performed with starting beam parameters listed in Table 1. The major contributing long-range collision regions are listed in Table 2. Note that the beam separation is several bunch widths at the $B0$ and $D0$ region where collisions would occur during high-energy physics operations. With chromaticity set to -2 units, and no beam-beam effect, the beams are clearly unstable as seen in Fig. 7. With beams separated, turning on the beam-beam effect prevents rapid oscillation growth during the simulation as shown in Fig. 8. The bursts of increased amplitude is sometimes indicative of the onset of instability, but it is not obvious

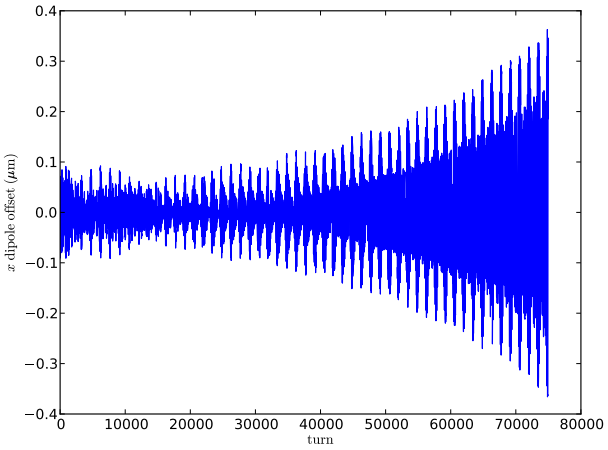

Figure 7. The x dipole moment in a simulation with $C = -2$ and no beam-beam effect showing the development of instability.

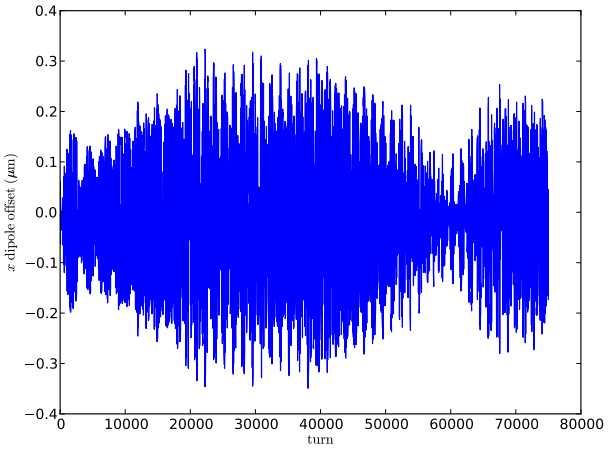

Figure 8. The x dipole moment of a representative bunch in a 36-on-36 simulation with $C = -2$ with beam-beam effects and beams separated showing no obvious instability within the limits of the simulation.

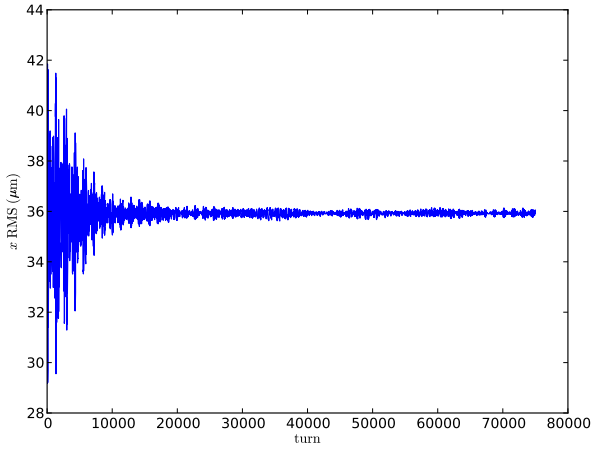

Figure 9. The x RMS moment of a representative bunch in a 36-on-36 simulation with $C = -2$ with beam-beam effects and beams separated showing no obvious instability within the limits of the simulation.

within the limited duration of this run. The RMS size of the beam also does not exhibit any obvious unstable tendencies as shown in Fig. 9.

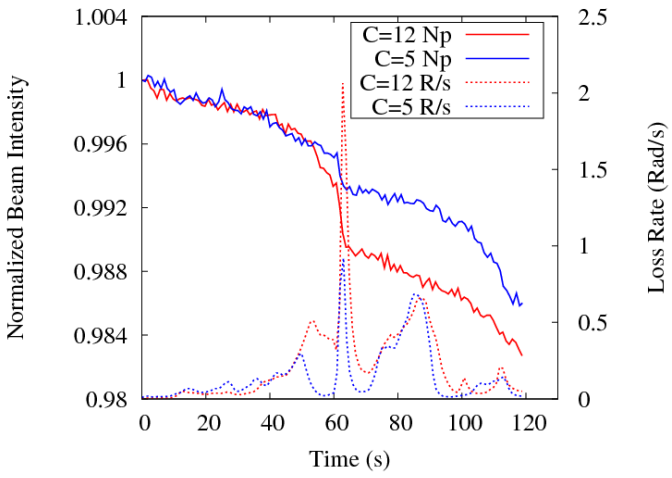

Figure 10. Plot of the beam current (solid line read with the left-hand scale) and radiation losses (dotted lines read with the right-hand scale) vs. time during the "squeeze" phase of setup for two values of chromaticity. The red curves are the values when running at a chromaticity $C = 12$ (the previously used high value) while the blue curves are for $C = 5$, the reduced chromaticity value. Lowering the chromaticity markedly prevents the drop in beam intensity around $t = 63$ and also lowers the radiation losses.

Based on these findings the chromaticity in the squeeze was lowered by a factor of two, and presently is kept at 8-9 units. This resulted in a 50% decrease in observed particle loss rates as shown in Fig. 10[18].

7. Summary

The key features of the simulation developed and improved under the SciDAC program include fully three-dimensional strong-strong multi-bunch beam-beam interactions with multiple interaction points, transverse resistive wall impedance, and chromaticity. The beam-beam interaction model has been shown to reproduce the location and evolution of synchrobetatron modes characteristic of the 3D strong-strong beam-beam interaction observed in experimental data from the VEPP-2M collider. The impedance calculation with macroparticles excites both the strong and weak head-tail instabilities with thresholds and growth rates that are consistent with expectations from a simple two-particle model and Vlasov calculation. Simulation of the interplay between the helical beam-orbit, long range beam-beam interactions and the collision pattern qualitatively matches observed patterns of emittance growth.

The new program is a valuable tool for evaluation of the interplay between the beam-beam effects and transverse collective instabilities. Simulations have been successfully used to support the change of chromaticity at the Tevatron, demonstrating that even the reduced beam-beam effect from long-range collisions may provide enough Landau damping to prevent the development of head-tail instability. These results were used in Tevatron operations to support a change of chromaticity during the transition to collider mode optics, leading to a factor of two decrease in proton losses, and thus improved reliability of collider operations.

Acknowledgments

We thank J. Qiang and R. Ryne of LBNL for the use of and assistance with the `BeamBeam3d` program. We are indebted to V. Lebedev and Yu. Alexahin for useful discussions. This work was supported by the United States Department of Energy under contract DE-AC02-07CH11359 and the ComPASS project funded through the Scientific Discovery through Advanced Computing program in the DOE Office of High Energy Physics. This research used resources of the National Energy Research Scientific Computing Center, which is supported by the Office of Science of the U.S. Department of Energy under Contract No. DE-AC02-05CH11231. This research used resources of the Argonne Leadership Computing Facility at Argonne National Laboratory, which is supported by the Office of Science of the U.S. Department of Energy under contract DE-AC02-06CH11357.

References

[1] US Particle Physics: Scientific Opportunities, Particle Physics Project Prioritization Panel, May 2008 available from `http://www.er.doe.gov/hep/files/pdfs/P5_Report%2006022008.pdf`.

[2] Run II handbook, http://www-bd.fnal.gov/runII

[3] Evidence for an anomalous like-sign dimuon charge asymmetry, arXiv:1005.2757 [hep-ex] http://arxiv.org/abs/1005.2757, submitted to Phys. Rev. D.

[4] T. Aaltonen et al., (CDF and D Collaborations), Combined CDF and D Upper Limits on Standard Model Higgs Boson Production in the W+W- Decay Mode, Phys. Rev. Lett. 104, 061802 (2010)

[5] E.A. Perevedentsev and A.A. Valishev, "Simulation of Head-Tail Instability of Colliding Bunches", Phys. Rev. ST Accel. Beams **4**, 024403, (2001)

[6] J. Qiang, M.A. Furman, R.D. Ryne, J.Comp.Phys., 198 (2004), pp. 278–294, J. Qiang, M.A. Furman, R.D. Ryne, Phys. Rev. ST Accel. Beams, 104402 (2002).

[7] V. Lebedev, http://www-bdnew.fnal.gov/pbar/ organizationalchart/lebedev/OptiM/optim.htm

[8] A. Valishev *et al.*, "Progress with Collision Optics of the Fermilab Tevatron Collider", EPAC06, Edinburgh, Scotland, 2006

[9] A. Chao, *Physics of Collective Beam Instabilities in High Energy Accelerators.*, pp. 56–60, 178–187, 333-360 John Wiley and Sons, Inc., (1993)

[10] I.N. Nesterenko, E.A. Perevedentsev, A.A. Valishev, Phys.Rev.E, 65, 056502 (2002)

[11] K. Yokoya, Phys. Rev. ST-AB **3**, 124401 (2000).

[12] A. Piwinski, IEEE Trans. Nucl. Sci. **NS-26** (3), 4268 (1979).

[13] E.A. Perevedentsev and A.A. Valishev, Phys. Rev. ST Accel. Beams 4, 024403 2001 ; in Proceedings of the 7th European Particle Accelerator Conference, Vienna, 2000 unpub- lished , p. 1223; http://accelconf.web.cern.ch/AccelConf/e00/ index.html

[14] V.V. Danilov and E.A. Perevedentsev, Nucl. Instrum. Methods Phys. Res. A 391, 77 1997 .

[15] A. Chao, *Physics of Collective Beam Instabilities in High Energy Accelerators.*, Figure 4.8 on p. 183, John Wiley and Sons, Inc., (1993).

[16] A. Chao, *Physics of Collective Beam Instabilities in High Energy Accelerators.*, p. 351, John Wiley and Sons, Inc., (1993).

[17] V. Shiltsev, *et al.*, "Beam-Beam Effects in the Tevatron," PRSTAB, **8**, 101001 (2005).

[18] A. Valishev *et al.*, "Recent Tevatron Operational Experience", PAC2009, Vancouver, BC, 2009